Rapid assessment of *S*-wave profiles from the inversion of multichannel surface wave dispersion data

G-Akis Tselentis and George Delis
University of Patras, Seismological Laboratory, Rio, Greece

Abstract
The importance of detailed knowledge of the shear-wave velocity structure of the upper geological layers was recently stressed in strong motion studies. In this work we describe an algorithm which we have developed to infer the 1D shear wave velocity structure from the inversion of multichannel surface wave dispersion data (ground-roll). Phase velocities are derived from wavenumber-frequency stacks while the inversion process is speeded up by the use of Householder transformations. Using synthetic and experimental data, we examined the applicability of the technique in deducing *S*-wave profiles. The comparison of the obtained results with those derived from cross-hole measurements and synthesized wave fields proved the reliability of the technique for the rapid assessment of shear wave profiles during microzonation investigations.

Key words *Rayleigh waves – shear wave profiles – site effects – microzonation*

1. Introduction

Many heavily developed regions of the world are in alluvial-filled valleys, and it has long been known from empirical observations that ground motions from earthquakes can be significantly altered by the near-surface geological materials in such regions (*e.g.*, Rovelli *et al.*, 1995; Chavez-Garcia *et al.*, 1995; Celebi, 1995).

Accurate shear wave velocity profiles have been long recognized as essential data to evaluate the dynamic response of soil deposits and soil-structure interaction under earthquake loading (Schnabel *et al.*, 1972). Thus, the rapid assessment of shear velocities as a function of depth is useful in analyzing the effect of site conditions on strong ground motion records and in estimating ground motion in future earthquakes for engineering purposes.

Boore *et al.* (1994) recently pointed out that the shear wave velocity structure within the first 30 m in depth is of critical importance in estimating strong ground motion at a site.

Despite the fact that the analytical methods used in earthquake engineering have improved substantially during the last two decades, the capability of determining soil properties *in-situ* has not followed this pattern. It is obvious that the use of very sophisticated constitutive models incorporated into large finite element programs often raises doubts about the final results where accurate soil properties are not available.

Surface wave dispersion analysis is one approach used to extract a subsurface 1D shear wave velocity model. In layered media, the ve-

Mailing address: Dr. G-Akis Tselentis, University of Patras, Seismological Laboratory, Rio 261 10, Greece; e-mail: Tselenti@upatras.gr

locity of propagation of surface waves depends on the wavelength of the wave and it is obvious that different wavelengths sample different sections of the layered media.

The advantage of obtaining shear wave velocity profiles by *in-situ* surface wave measurements has been recognized since the 1960's when Jones (1962) and Ballard (1964) developed the first measurement systems. Since then, several researchers have developed and improved the techniques for surface wave measurements.

Szelwis and Behle (1984) used multi-modal Rayleigh waves to determine shear wave velocities in shallow structures and Jongmans and Demanet (1993) showed the importance of surface wave analysis for the estimation of dynamic characteristics of soils. Stokoe and Nazarian (1983), Tselentis and Delis (1990), Roesset *et al.* (1991) and Gucunski and Woods (1991) developed, among others, techniques based on the spectral analysis of surface waves to be used in geophysical prospecting.

Generally, a dispersion curve is a nonlinear function of shear wave velocities, densities and thicknesses for each layer. To invert a dispersion curve into these parameters, a linearized approximation is usually used by neglecting higher order terms in the Taylor series expansion. Then, an optimal solution is obtained by an interactive perturbation process based on linear inverse theory.

2. Principle of the method

Various studies have shown that the linearized inversion is connected with many numerical difficulties when dealing with noisy data. Furthermore, a final inverted model determined by a linearized inversion inherently depends on an assumed initial model, because of the existence of locally optimal solutions (Yamanaka and Ishida, 1996). It is obvious that for the upper sedimentary layers, which are the target of the present investigation, it is sometimes difficult to set up an initial model that is sufficiently close to the real solution. In this case it is common for the inversion to find a local rather than a global minimum. The two principal stages of the technique are: 1) evaluation of phase velocity dispersion and 2) inversion for shear wave structure.

2.1. *Evaluation of dispersion by k-f stacking*

An important aspect which determines the accuracy of the present methodology is the evaluation of the field dispersion curve from multichannel data.

McMechan and Yedlin (1981) described a method to obtain phase velocity from a dispersion wave in a common shot gather. The method consists of performing a slant stack on the data to obtain a wave field in the p-τ domain, followed by a 1D Fourier transform over τ to obtain the wavefield in the (slowness) p-ω plane.

The approach which we followed is similar to the p-ω stacking technique of McMechan and Yeldin (1981) but instead of the slowness (p)-ω domain we work on the wavenumber (k)-f domain.

Assuming vertical heterogeneity only, the complete normal mode solution of surface wave propagation can be written as (Aki and Richards, 1980)

$$s(x, t) = \frac{1}{2\pi} \int_{-\infty}^{\infty} \sum_{m} S_m(\omega, x)\, e^{i(\omega t - k_m(\omega) x)} d\omega \qquad (2.1)$$

where

$$S_m(\omega, x) = I(\omega)\, P_m(\omega)\, R_m(\omega) \frac{e^{-\gamma_m(\omega) x}}{\sqrt{x}} \qquad (2.2)$$

and

m = mode number;
$I(\omega)$ = instrument response;
$P_m(\omega)$ = source spectrum;
$R_m(\omega)$ = path response;
$\gamma_m(\omega)$ = attenuation coefficient.

Let N be spatially separated (by Δx) geophones at the same azimuth as the seismic source. The usual p-τ (slant) stacking method (Dziewonski and Hales, 1972; McMechan and Yedlin, 1981) involves searching all traces for phase velocities that will produce constructive interference of monochromatic waves at a given frequency.

Assuming that the phase offset between any two geophones can be described as $k_m(\omega)\Delta x$ and the wavenumber is related to the phase velocity ($c_m(\omega)$) and the slowness $p_m(\omega)$ as

$$k_m(\omega) = \frac{\omega}{c_m(\omega)} = \omega p_m(\omega) \qquad (2.3)$$

we perform the following slant stack

$$\sum_{n=1}^{N} s(x_n, \tau + p x_n) =$$

$$= \sum_{n=1}^{N} \frac{1}{2\pi} \int_{-\infty}^{\infty} \sum_{m=1}^{N} S_m(\omega, x_n)\, e^{i(\omega\tau + \omega p x_n - k_m(\omega) x_n)}\, d\omega =$$

$$= \frac{1}{2\pi} \int_{-\infty}^{\infty} e^{i\omega\tau} \sum_{m=1}^{M} \sum_{n=1}^{N} S_m(\omega, x_n)\, e^{i(\omega p - k_m(\omega)) x_n}\, d\omega. \qquad (2.4)$$

Compensating for attenuation and taking the Fourier transform of (2.4) we obtain the equation

$$F(f, k) = \sum_{m=1}^{M} S_m(f) \left[\sum_{n=1}^{N} e^{-\gamma_m(f) x_n} e^{i(k - k_m(f)) x_n} \right]. \qquad (2.5)$$

Setting the (resolution) function within the brackets as W_m, the modulus of (2.5) can be written as

$$|F(f, k)| = \sum_{m=1}^{M} |S_m(f)|\,|W_m(k - k_m(f))|. \qquad (2.6)$$

Plotting (2.6) as a two dimensional function of k and f and tracing the maxima we can easily assess the phase velocity as a function of frequency. It can be shown (Appendix 1) that the modulus of the resolution function W_m is given by

$$|W_m| =$$

$$= e^{-\gamma_m(f) X} \left(\frac{\sin^2\left([k - k_m(f)]\frac{N\Delta x}{2}\right) + \sinh^2\left(\gamma_m(f)\frac{N\Delta x}{2}\right)}{\sin^2\left([k - k_m(f)]\frac{\Delta x}{2}\right) + \sinh^2\left(\gamma_m(f)\frac{\Delta x}{2}\right)} \right)^{1/2} \qquad (2.7)$$

where

$$X = x_0 + (N - 1)\Delta x/2.$$

This result shows that W_m is a periodic function with period $N/(f\Delta x)$. Differentiating (2.7) with respect to k and setting the result to zero we obtain the maximum when $k = k_m(f)$. Thus, attenuation has no effect on the position of the maximum and hence the accuracy of tracing the phase velocity dispersion curve (Russell, 1987).

The benefit of working on the k-f domain is that the assessed dispersion curves are smoother, and this certainly facilitates the inversion procedure which will be described in the next section.

2.2. *Formulation of the inverse problem*

The obtained dispersion data, combined with an initial model were used to invert for the shear velocity structure. The formulation of the inverse problem will be performed adopting variational analysis (Russell, 1987), by calculating first order perturbations in the eigenvalues of normal mode equations.

The parameters of the initial model are set by the following empirical relations which have been found in most of the cases to produce stable results

$$d_i = \frac{1}{4\pi} \ln(\lambda) \tag{2.8}$$

$$V_{si} = f\lambda \frac{i}{i+1} \pi^2 \tag{2.9}$$

$$\rho_i = 1.2\left(1 + \frac{i-1}{N-1}\right) \tag{2.10}$$

where d_i, V_{si}, ρ_i is the corresponding thickness, shear velocity and density of layer i and N the number of layers.

The equation of Rayleigh wave motion is given by the following system of equations (Aki and Richards, 1980, eq. (7.28))

$$\frac{d}{dz}\begin{bmatrix} r_1 \\ r_2 \\ r_3 \\ r_4 \end{bmatrix} =$$

$$= \begin{bmatrix} 0 & -k & \mu^{-1} & 0 \\ k\lambda(\lambda+2\mu)^{-1} & 0 & 0 & (\lambda+2\mu)^{-1} \\ k^2\zeta - \omega^2\rho & 0 & 0 & -k\lambda(\lambda+2\mu)^{-1} \\ 0 & -\omega^2\rho & k & 0 \end{bmatrix} \begin{bmatrix} r_1 \\ r_2 \\ r_3 \\ r_4 \end{bmatrix} \tag{2.11}$$

where

ζ = $4\mu(\lambda+\mu)/(\lambda+2\mu)$;
λ, μ = Lame constants;
r_1, r_2 = radial and vertical displacement eigenfunctions;
r_3, r_4 = radial and vertical stress eigenfunctons;
ρ = density.

Solving the first and second rows of eq. (2.11) for r_3, r_4 and substituting into the third and fourth rows, after some rearrangement, we obtain forms explicitly dependent on displacement eigenfunctions only. We can write (Appendix 2)

$$\frac{d}{dz}\left(A\frac{dr}{dz} + kBr\right) = kB^T\frac{dr}{dz} + k^2Cr - \omega^2\rho r \tag{2.12}$$

where A, B, C and r are defined as:

$$A = \begin{bmatrix} \mu & 0 \\ 0 & (\lambda+2\mu) \end{bmatrix}$$

$$B = \begin{bmatrix} 0 & \mu \\ -\lambda & 0 \end{bmatrix}$$

$$C = \begin{bmatrix} (\lambda+2\mu) & 0 \\ 0 & \mu \end{bmatrix}$$

$$r = \begin{bmatrix} r_1 \\ r_2 \end{bmatrix}$$

Equation (2.12) is self adjointing in the interval $(0, \infty)$ thus, the basic principles of variational analysis can be applied resulting in the following relations (Appendix 2)

$$\delta c(f) = \int_0^\infty A_R(f, z)\, \delta\beta(z)\, dz \tag{2.13}$$

where

$$A_R(f, z) = \frac{\mu c}{\beta k U}\left[\left(kr_2 + \frac{dr_1}{dz}\right)^2 + 4kr_1\frac{dr_2}{dz}\right] \tag{2.14}$$

and

$$U = 2k\int_0^\infty [(\lambda+2\mu)r_1^2 + \mu r_2^2]\, dz + \int_0^\infty \left(\mu r_2\frac{dr_1}{dz} - \lambda r_1\frac{dr_2}{dz}\right) dz. \tag{2.15}$$

The above equations relate perturbations in structural velocity and density to observed phase velocities at the free surface. Assuming a starting earth model of velocities and densities, as previously described, perturbations in phase velocities (δc) can be assessed by subtracting the theoretical phase velocities from observed velocities. Holding compressional velocity and density fixed and inverting the above integral equations for $\delta\beta$, estimates for shear velocity can be determined as functions of δc. Equation (2.13) can be written in the following vector form

$$[\delta c] = [A]\,[\delta\beta] = [A]T^{-1}T[\delta\beta] \qquad (2.16)$$

where T is the Householder transformation (Menke, 1989). We have found that by adopting this approach we end up with a stable and accurate inversion process which can be easily performed with a common laptop at the site of investigation. A numerical code on *C* has been developed to perform all the previously mentioned calculations.

After evaluating the theoretical dispersion curve we increase the corresponding data points by cubic spline interpolation and overall smoothing. This process can be considered as adding to the problem *a priori* information by including new data in new frequency coordinates. Eventually we end up with an even-determined problem to solve. Figure 1 depicts the various stages of the inversion process.

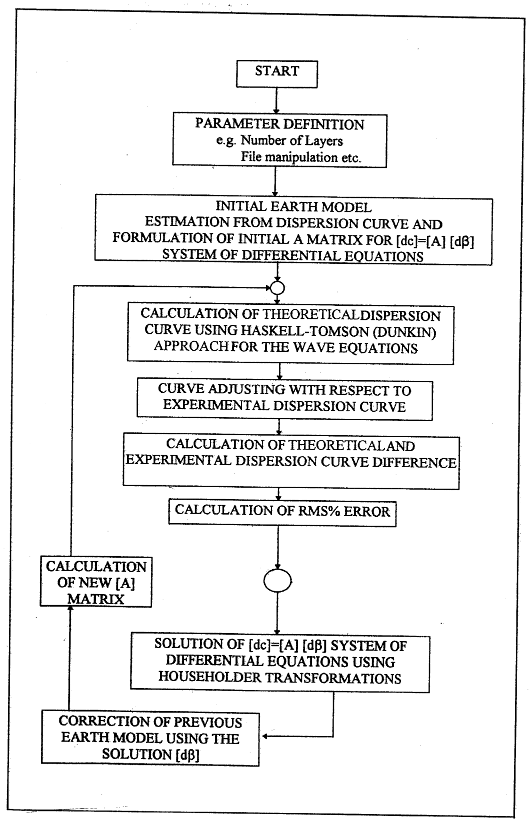

Fig. 1. Data processing followed during the inversion.

3. Inversion of synthetic data

To test the accuracy of the inversion methodology, a finite-difference method was employed to simulate the generation and propagation of short-period Rayleigh waves for a known geological model. We start from an *S*-wave velocity profile (30 m of 500 m/s over half space of 800 m/s) and generate surface wave synthetic seismograms. The synthetics were calculated, using the finite difference algorithm of Zahradnik (1995).

The calculations performed in this study are for the vertical component motion due to a vertical body force at the surface. The time variation of the force is a Gabor wavelet (50 Hz). The generated synthetics are shown in fig. 2. The inverted shear velocity model is shown in fig. 3 and is compared with the theoretical model for various iterations. It is obvious that there is a satisfactory comparison between the actual and assessed model.

The corresponding theoretical and calculated dispersion curves are depicted in fig. 4, indicating a satisfactory agreement and verifying the accuracy of the inversion process. The calculated isoline representation of the *k-f* stack as a function of frequency and phase velocity is shown in fig. 5.

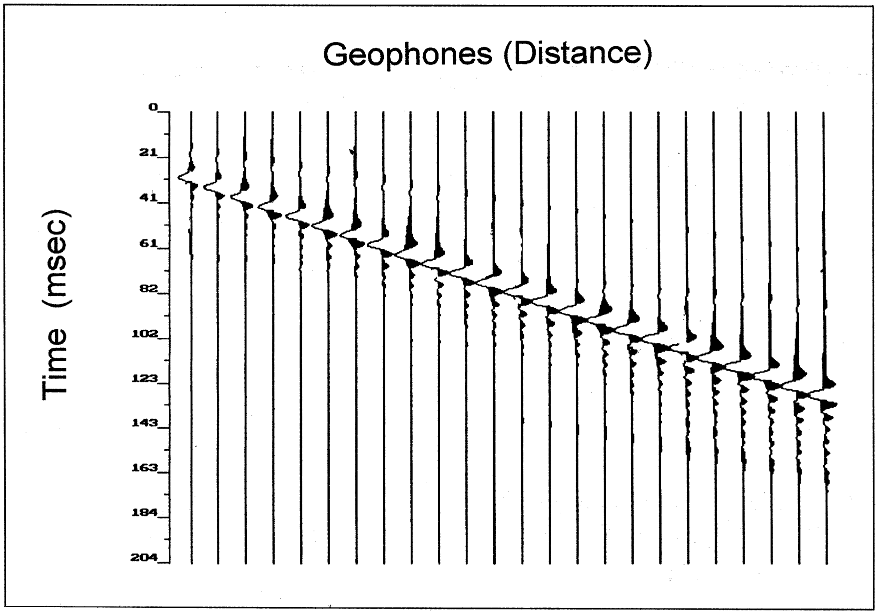

Fig. 2. Synthetic seismograms.

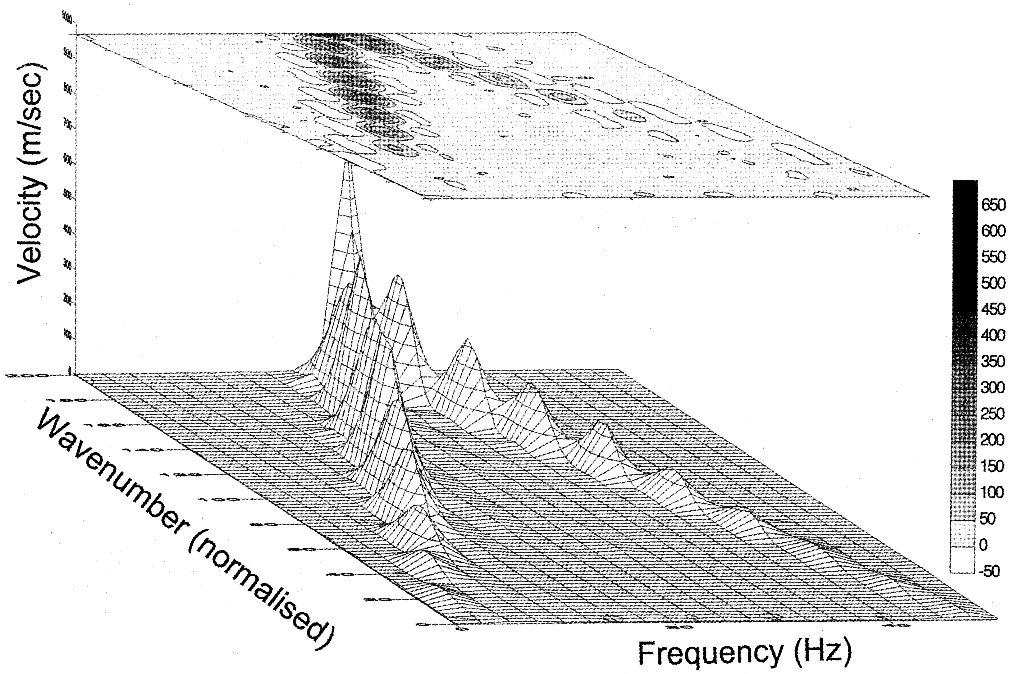

Fig. 3. Isoline representation of *k-f* stack as a function of frequency and phase velocity for synthetic data.

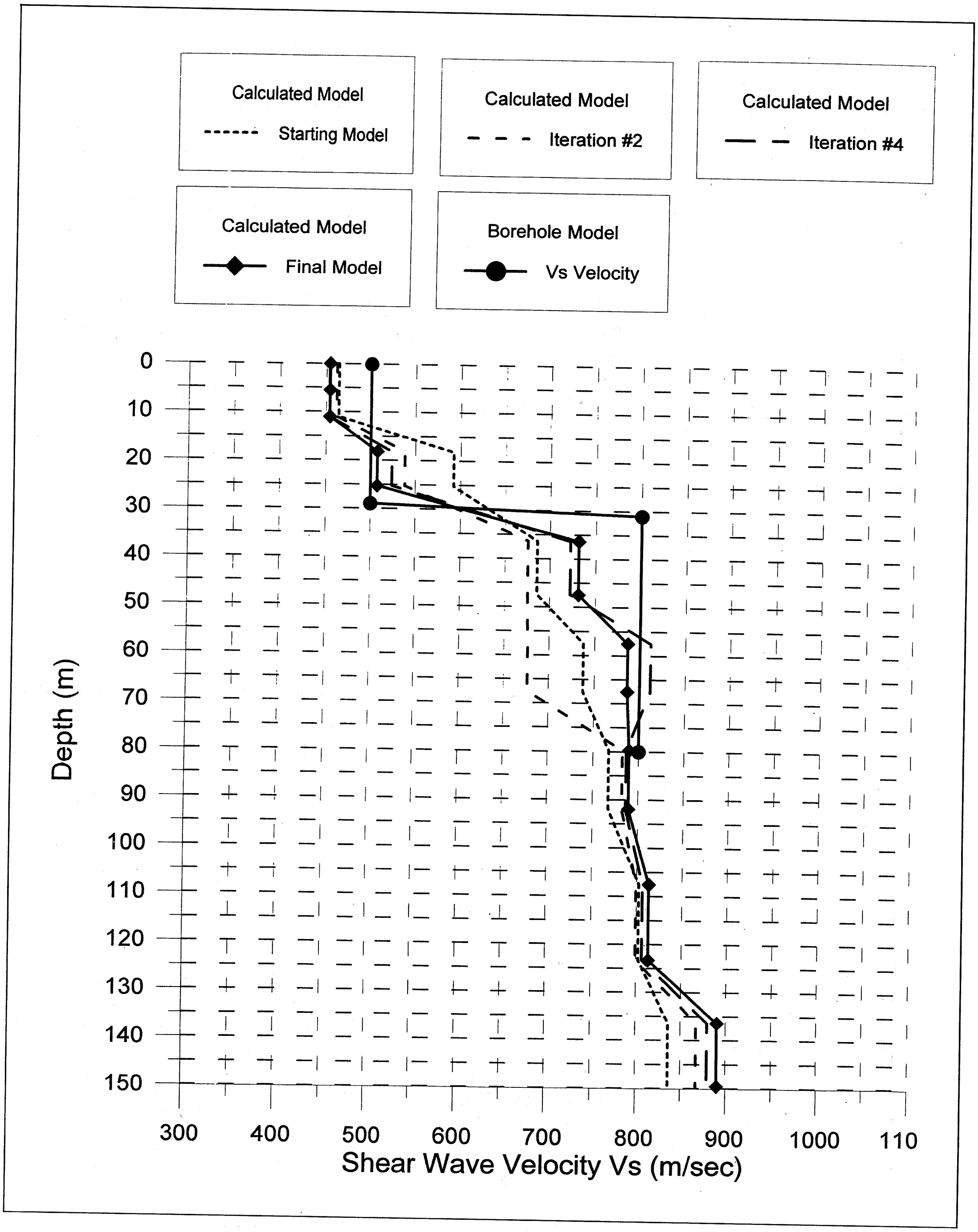

Fig. 4. Comparison of synthetic model with the calculated one.

4. Inversion of observed data

Each data trace consists of 5 s of digital data with a sampling interval of 5 ms. Twenty four 1 Hz vertical geophones were used. In most cases all traces from a given side of the seismic source are used to obtain an average velocity structure for that side. Thus, small lateral heterogeneities are averaged.

A critical parameter of the field procedure is the distance of the seismic source to the first geophone, since dispersion starts to develop several wavelengths from the seismic source.

As a seismic source we used a BISON EWGII elastic wave generator with which we have reached exploration depths up to 200 m. We have also obtained good results with impacts by a hammer but the depth of investi-

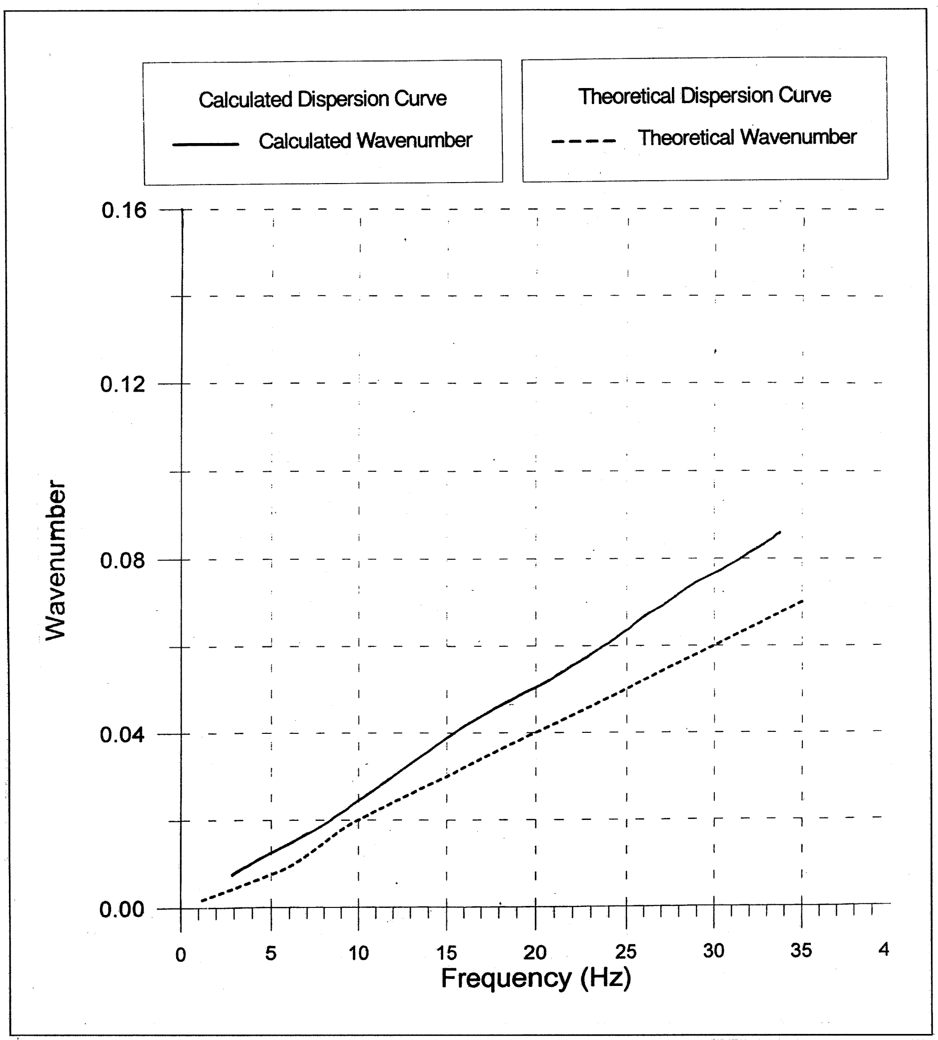

Fig. 5. Comparison of calculated and theoretical dispersion curves for synthetic data.

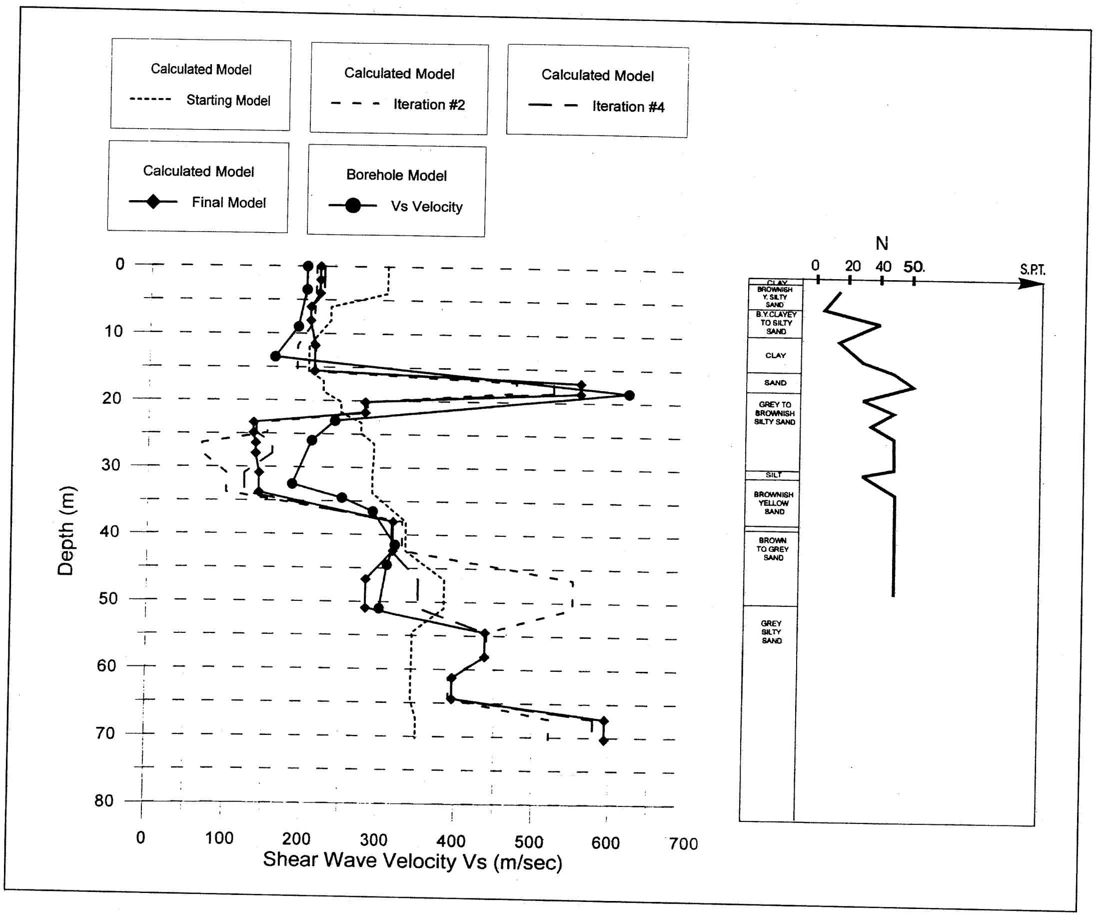

Fig. 6. Results from cross-hole and SPT measurements and comparison with calculated by applying the developed methodology.

gation was reduced to a few tenths of meters.

A borehole was drilled to a depth of about 80 m. The soil samples were subjected to classification tests. The obtained lithologic section is depicted in fig. 5. Standard Penetration Tests (SPT) at 1.5 m intervals were also performed and the SPT mechanism, rich in shear wave energy was also used as a mechanical impulse source for cross-hole measurements in a nearby borehole. The measured shear wave velocities and the SPT values are depicted in fig. 6. The existence of a sandy layer at a depth of about 15 m is obvious.

The recorded seismograms are shown in fig. 7. Isoline representation of the *k-f* stack as a function of frequency and phase velocity is shown in fig. 8. It is obvious that a strong fundamental mode dominates the observed waveforms.

Figure 9 shows the corresponding calculated and theoretical dispersion curves. A comparison between the velocity inversion results and the geological model (fig. 6), indicates good resolution in defining the various geotechnical entities and a close agreement with the cross-hole results.

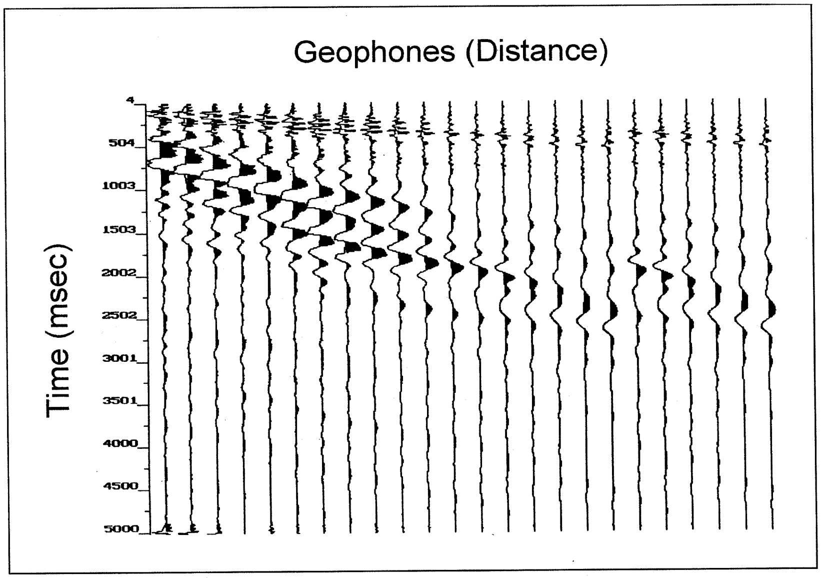

Fig. 7. Observed seismograms.

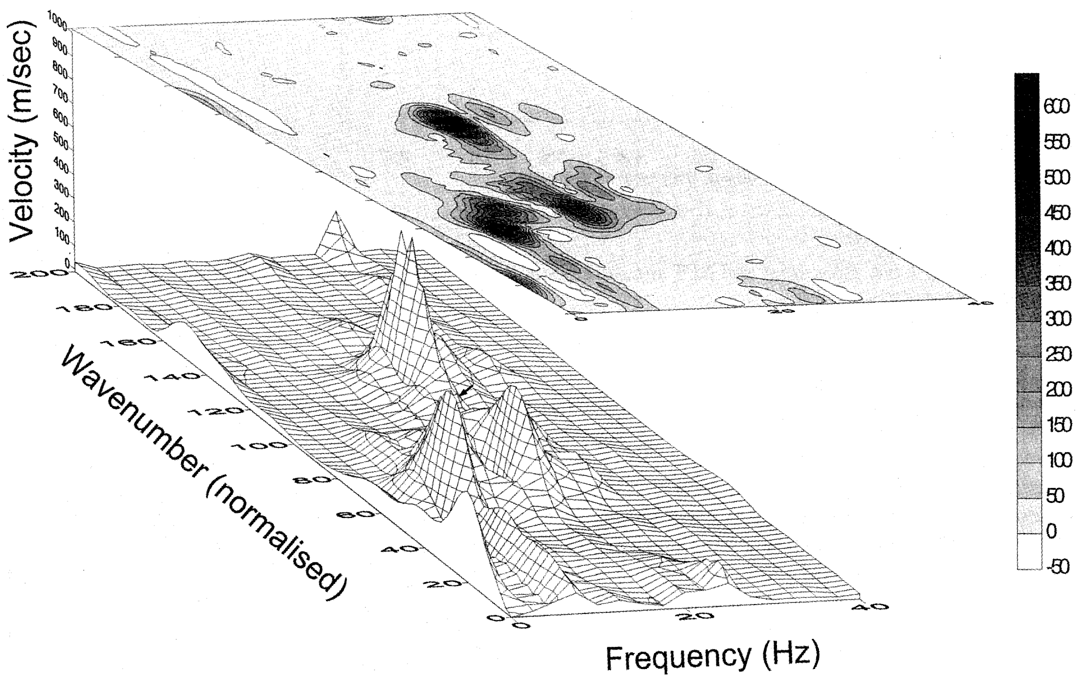

Fig. 8. Isoline representation of *k-f* stack as a function of frequency and phase velocity for measured data. Vector indicates fundamental mode.

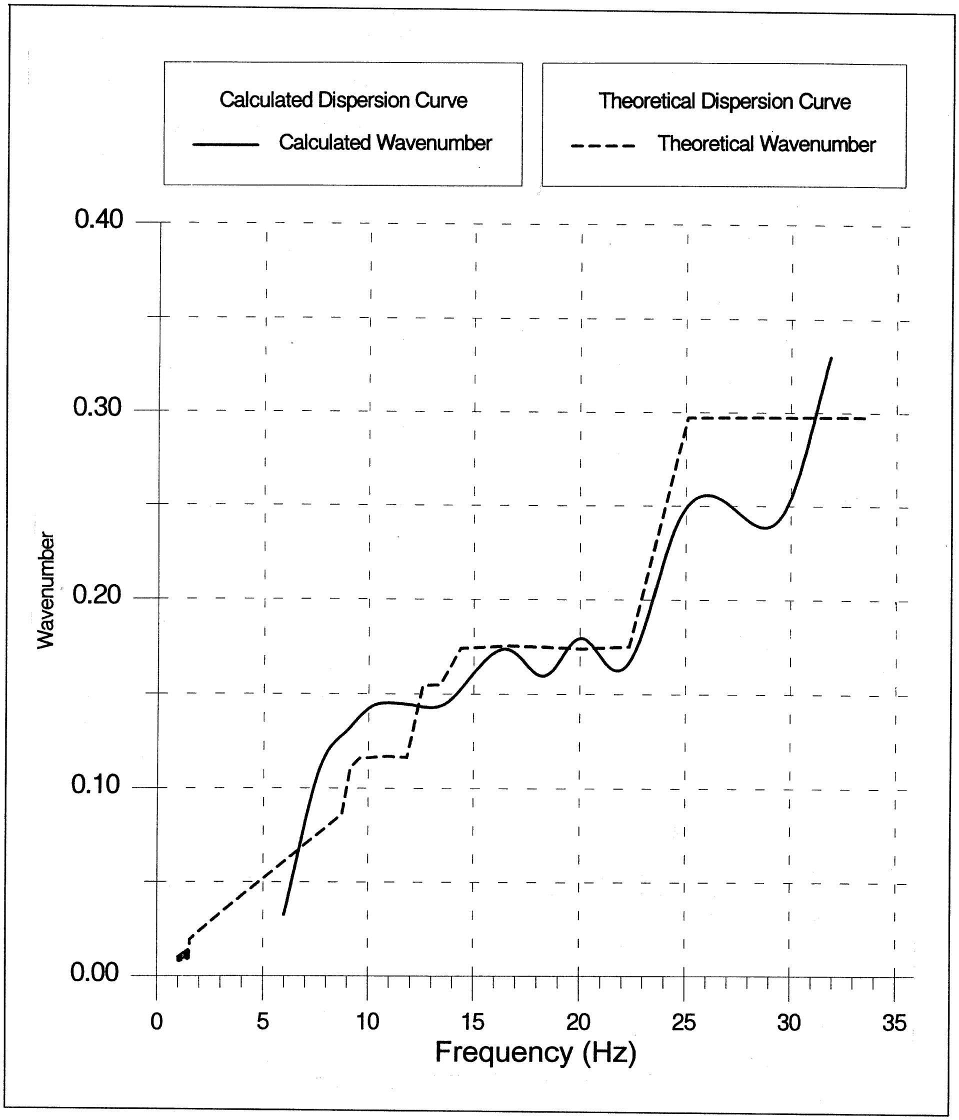

Fig. 9. Comparison of calculated and theoretical dispersion curves for field data.

5. Conclusions

A method for determining *S*-wave profiles of the upper geological layers, using artificially generated short period Rayleigh waves (ground roll) has been presented in this study.

By using wavenumber-frequency stacks to assess the phase velocity dispersion curve and Householder transformation to speed up the inverse problem an algorithm has been developed suitable to be incorporated in almost all PC-based engineering seismographs.

Shear velocity profiles obtained using the method show a good correlation with results from verification borings and direct cross-hole shear wave velocity measurements.

The method can be easily applied for studying the lateral variation of shallow shear-wave velocity which is a critical parameter during microzonation investigations.

Acknowledgements

This work was partially supported by the public works laboratory (KEDE) of Greece and NATO sfs GR-Coal project. The authors would like to thank Dr. D. Russell for supplying useful information concerning his Ph.D. work and Dr. J. Zahradnik for making available to us his finite difference code to generate the synthetic case history. We also thank Mrs. J. Vasiliou and Mr. D. Rubas for their help during the geotechnical and geophysical investigations. The comments of two anonymous reviewers proved extremely helpful.

REFERENCES

AKI, K. and P.G. RICHARDS (1980): *Quantitative Seismology-Theory and Methods* (Freeman, San Francisco).

BALLARD, R.F. (1964): Determination of soil shear moduli at depth by *in-situ* vibratory techniques, U.S. Army Enginers Waterways Experiment Station, Vicksburgh, Mississippi, *miscellaneous paper* No. 4-691.

BOORE, D.M., W.B. JOYNER and T.E. FUMAL (1994): Estimation of response spectra and peak accelerations from Western North American earthquakes, an interim report, part 2, *U.S. Geol. Surv. Open-File Rept.* 94-127.

BUTKOV, E. (1968): *Mathematical Physics* (Addison-Wesley Publ. Inc., Massachusetts), pp. 637.

CELEBI, M. (1995): Northridge (California) earthquake: unique ground motions and resulting spectra and site effects, in *Proceedings 5th International Conference on Seismic Zonation, Nice, France*, vol. 1, 988-995.

CHAVEZ-GARCIA, F.J., J. CUENCA and J. LERMO (1995): Seismic microzonation in Mexico. The examples of Mexico City Oaxaca and Puebla, in *5th Proceedings International Conference on Seismic Zonation, Nice, France*, vol. 1, 699-706.

DZIEWONSKI, A.M. and A.L. HALES (1972): Numerical analysis of dispersed seismic waves, in *Methods in Computational Physics*, edited by B.A. BOLT, vol. II, 39-85.

GUCUNSKI, N. and R.D. WOODS (1991): Inversion of Rayleigh wave dispersion curve for SASW test, in *Proceedings of the Fifth International Conference on Soil Dynamics and Earthquake Engineering, SDEE 91, Karlsruhe, Germany, 23-26 September 1991*, 127-138.

JONES, R. (1962): Surface wave technique for measuring the elastic properties and thickness of roads, *Br. J. Appl. Phys.*, **13**, 21-29.

JONGMANS, D. and D. DEMANET (1993): The importance of surface vibration study and the use of Rayleigh waves for estimating the dynamic characteristics of soils, *Eng. Geol.*, **34**, 105-113.

MCMECHAN, G.A. and M.J. YEDLIN (1981): Analysis of dispersive waves by wave field transformation, *Geophysics*, **46**, 869-874.

MENKE, W. (1989): *Geophysical Data Analysis: Discrete Inverse Theory* (Academic Press Inc., San Diego), pp. 378.

ROESSET, J.M., D.W. CHANG and K.H. STOKOE (1991): Comparison of 2D and 3D models for analysis of surface wave tests, in *Proceedings of the Fifth International Conference on Soil Dynamics and Earthquake Engineering, SDEE 91, Karlsruhe, Germany, 23-26 September 1991*, 111-126.

ROVELLI, A., L. MALAGNINI, A. CASERTA and F. MARRA (1995): Using 1 and 2D modeling of ground motion for seismic zonation criteria: results from the city of Rome, *Ann. Geofis.*, **38**, 591-605.

RUSSELL, D.R. (1987): Multichannel processing of dispersed surface waves, *Ph.D. Thesis*, Saint Louis University.

SCHNABEL, P.B, J. LYSMER and H.B. SEED (1972): SHAKE - A computer program for earthquake response analysis of horizontally layered sites, EERC 72-12.

STOKOE, K.H. and S. NAZARIAN (1983): Effectiveness of ground improvement from spectral analysis of surface waves, in *Proceedings of the Eighth European Conference on Soil Mechanics and Foundation Engineering, Helsinki, Finland, May 1983*, 157-172.

SZELWIS, R. and A. BEHLE (1984): Shallow shear-wave velocity estimation from multi-modal Rayleigh waves, in *Shear-Wave Exploration*, edited by S.H. DANBOM and S.N. DOMENICO, *Geophysical Development Series*, vol. 1, SEG, 214-226.

TSELENTIS, G-A. and G. DELIS (1990): *In situ* rapid assessment of dynamic soil characteristics for microzonation investigations, in *Proceedings of the Sixth International IAEG Congress, Rotterdam* (Balkema Publ.), 893-897.

YAMANAKA, H. and H. ISHIDA (1996): Application of genetic algorithms to an inversion of surface-wave dispersion data, *Bull. Seism. Soc. Am.*, **86** (2), 436-444.

ZAHRADNIK, J. (1995): Simple elastic finite-difference scheme, *Bull. Seism. Soc. Am.*, **85**, 1879-1887.

(received July 15, 1997;
accepted February 10, 1998)

Appendix 1. Proof of eq. (2.7).

The modulus of the resolving function can be expressed as:

$$|W_m| = \left|\sum_n\right| e^{Z_m X_n}. \tag{A.1.1}$$

Where

$$Z_m = -\gamma_m(f) + i\,[k - k_m(f)]. \tag{A.1.2}$$

If the seismic source is at a distance x_0 from the first geophone we can write:

$$|W_m| = e^{-\gamma_m(f)x_0}\left|\frac{e^{Z_m N\Delta x} - 1}{e^{Z_m \Delta x} - 1}\right| = \tag{A.1.3}$$

$$= e^{-\gamma_m(f)x_0}\left| e^{\left[Z_m (N-1)\frac{\Delta x}{2}\right]} \frac{\sin\left(Z_m \frac{N\Delta x}{2}\right)}{\sin\left(Z_m \frac{\Delta x}{2}\right)}\right|$$

which, when we consider the modulus of the complex sine function becomes eq. (2.7).

Appendix 2. Proof of eq. (2.12).

Consider the following set of linear differential equations

$$Lu = \sum_j k^j M_j u. \tag{A.2.1}$$

From classical variational theory we can write (*e.g.*, Butkov, 1968)

$$\delta k = \frac{1}{U}\int_z u^T(\delta L u - \sum_j k^j \delta M_j u)\,dz \tag{A.2.2}$$

where

L, M = linear differential operators;
k = eigenvalue found at f;
u = vector of eigenfunctions.

Let $L = \frac{d}{dz}A\frac{d}{dz}$, $M_0 = -\omega^2\rho$, $M_1 = \left(B^T\frac{d}{dz} - \frac{dB}{dz}\right)$, $M_2 = C$. Substituting these values into eq. (2.12) gives an exactly equivalent form to (A.2.1). So we can adopt that the integral (A.2.2) is a valid expression for eigenvalue perturbation in our case. Substituting into the integral we obtain

$$\delta k \int_0^\infty \left(r^T B^T \frac{dr}{dz} - r^T \frac{dBr}{dz} + 2\,k\,r^T Cr \right) dz = \\ = \int_0^\infty \left[r^T \frac{d}{dz}\left(\delta A \frac{dr}{dz} \right) + r^T r \omega^2 \delta\rho - kr^T \delta B^T \frac{dr}{dz} + kr^T \frac{d\delta Br}{dz} - k^2 r^T \delta Cr \right] dz. \tag{A.2.3}$$

Integrating by parts we can write

$$\delta k \int_0^\infty \left(2r^T B^T \frac{dr}{dz} + 2\,k\,r^T Cr \right) dz = r^T \left(\delta A \frac{dr}{dz} + k\delta Br + \delta k\, Br \right) \Big|_0^\infty + \\ + \int_0^\infty \left[-\frac{dr^T}{dz} \delta A \frac{dr}{dz} + r^T r \omega^2 \delta\rho - 2\,k\,r^T \delta B^T \frac{dr}{dz} - k^2 r^T \delta Cr \right] dz. \tag{A.2.4}$$

Setting

$$U = 2k \int_0^\infty [(\lambda + 2\mu)\, r_1^2 + \mu\, r_2^2]\, dz + 2 \int_0^\infty \left(\mu r_2 \frac{dr_1}{dz} - \lambda\, r_1 \frac{dr_2}{dz} \right) dz$$

$$U \delta k = \omega^2 \int_0^\infty \delta\rho\, (r_1^2 + r_2^2)\, dz - k^2 \int_0^\infty [\delta(\lambda + 2\mu)\, r_1^2 + \delta\mu\, r_2^2]\, dz \; - \\ -2\,k \int_0^\infty \left(\delta\mu\, r_2 \frac{dr_1}{dz} - \delta\lambda\, r_1 \frac{dr_2}{dz} \right) dz - \int_0^\infty \left[\delta\mu \left(\frac{dr_1}{dz} \right)^2 + \delta(\lambda + 2\mu) \left(\frac{dr_2}{dz} \right) \right] dz \tag{A.2.5}$$

which is simplified as

$$\delta k = \frac{1}{U} \int_0^\infty \omega^2 (r_1^2 + r_2^2)\, \delta\rho\, dz - \\ - \frac{1}{U} \int_0^\infty \left[\left(kr_1 - \frac{dr_2}{dz} \right)^2 \delta(\lambda + 2\mu) + \left(\left(kr_2 - \frac{dr_1}{dz} \right)^2 + 4kr_1 \frac{dr_2}{dz} \right) \delta\mu \right] dz. \tag{A.2.6}$$

Since

$$(\lambda + 2\mu) = \alpha^2 \rho, \; \mu = \beta^2 \rho \text{ and } c = \omega / k$$

$$\frac{\delta(\lambda + 2\mu)}{(\lambda + 2\mu)} = 2\frac{\delta\alpha}{\alpha} + \frac{\delta\rho}{\rho} \tag{A.2.7}$$

$$\frac{\delta\mu}{\mu} = 2\frac{\delta\beta}{\beta} + \frac{\delta\rho}{\rho} \tag{A.2.8}$$

$$\frac{\delta c}{c} = -\frac{\delta k}{k}. \tag{A.2.9}$$

These are the first order perturbations, which when substituted into (A.2.6) result

$$
\begin{aligned}
\delta c = {} & \frac{c}{kU}\int_0^\infty \left(kr_1 - \frac{dr_2}{dz}\right)^2 2\,(\lambda + 2\mu)\,\frac{\delta\alpha}{\alpha}\,dz + \\
& + \frac{c}{kU}\int_0^\infty \left[\left(kr_2 + \frac{dr_1}{dz}\right)^2 + 4kr_1\frac{dr_2}{dz}\right] 2\mu\,\frac{\delta\beta}{\beta}\,dz + \\
& + \frac{c}{kU}\int_0^\infty \left(kr_1 - \frac{dr_2}{dz}\right)^2 (\lambda + 2\mu)\,\frac{\delta\rho}{\rho}\,dz + \\
& + \frac{c}{kU}\int_0^\infty \left[\left(kr_2 + \frac{dr_1}{dz}\right)^2 + 4kr_1\frac{dr_2}{dz}\right] \mu\,\frac{\delta\rho}{\rho}\,dz.
\end{aligned}
\qquad \text{(A.2.10)}
$$

This equation, which is equivalent to eq. (2.13), defines the inverse problem to be solved.